Mapping saline soils using Hyperion hyperspectral images data in Mleta plain of the Watershed of the great Oran Sebkha (West Algeria)

Dif Amar[1], BENALI Abdelmadjid[2], BERRICHI Fouzi[3]

[1,3]Earth observation division, Center of space techniques, Arzew, Oran, Algeria
[2]Hydrogeology department, University of Oran 2 Ahmed ben ahmed, Oran, Algeria

Abstract— *The hyperspectral optical imagery constitutes a significant mine of information. These images reveal valuable information about soil conditions and can be used successfully in the saline soils mapping domain.*
Currently, the use of spatial hyperspectral image is considered to be a most spectacular technological revolution, because it has the advantage to reconstruct almost the entire spectrum of each images pixel. This characteristic, which is connected to the large number of bands, is achieved at the expense of the size of the image swath on the ground.
Only one scene satellite Hyperion image composed of more than two hundred twenty (220) images was used to cover the central part of the Mleta plain. These images are corrected on radiometric and atmospheric plan. The atmospheric corrections are made by FLAASH module using the MODTRAN radiative transfer model. This operation will subtract the values of absorbed radiation and layers atmospheric backscattered to find in the end the true reflectance values at ground level. The classification, based on almost continuous spectral information of the thematic objects across the electromagnetic spectrum, applied on these images will allow highlighting the different saline soils classes.

Two mapping methods have been used to mapping salinity. The first method is made from a colored composition between the first MNF (Minimum Noise Fraction) images. As for the second, it is done using a SAM (Spectral Angle Mapper) classification method based on information contained in the various spectral calculated from the image and compared with those of the spectral library.

Keywords— Saline Soil, Hyperspectral Image, EO-1 Hyperion Satellite, Mleta Plain.

I. INTRODUCTION

The evolution of airborne hyperspectral sensors has enriched the spaceport and space remote sensing images of more and more precise and detailed. The Hyperspectral remote sensing provides medium resolution images with fine spectral range in the visible and infrared. With a wide spectral range, the hyperspectral data has seen expansions in earth observation in civil and defense applications.

The Hyperion sensor images are obtained through an spectro-imager. The acquisition of a same scene is completed in the two hundred forty two (242) spectral bands. These bands form a quasi-continuous reflectance spectrum for each object on image. The first seventy (70) bands cover the spectrum of the visible and near infrared (356nm-1058 nm) and one hundred seventy two (172) bands in the short wavelength infrared (852nm-2577nm). From the set of bands (242), only one hundred ninety eight (198) bands are calibrated. It's due to overlap between bands of the visible and infrared, it remains only 196 unique channels. The calibrated channels are (8-57) for the visible and near-infrared and (77-224) for the average infrared channels.

II. GEOGRAPHIC SITUATION OF STUD AREA

The plain of Mleta is located in the South West of the Oran city (Fig. n ° 1). It occupies the southern part of the endorheic basin of the great Oran Sebkha. The basin is inserted between two mountains sets, the Tessala mountain in the South, culminating at 1061 meters (peak of Tessala) and the Murdjadjo mountain in the North, culminating at 584 meters.

Geographically the plain of the Mleta is located between 3G 25' and 3G 71' longitudes and latitudes 39G 21' and 39G 54'. It's bounded to the North by the great Oran Sebkha, to the South by the Tessalas mountains, East by Tlelat plain and to the West by the basin of Oued El Mellah

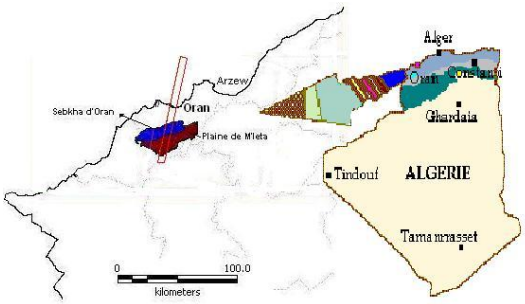

FIG. 1: LOCATION OF THE STUDY AREA

III. HYPERSPECTRAL DATA PRESENTATION

Use either The mode of spatial representation of multispectral remote sensing images in the three color components is easily achievable. In turn, hyperspectral data composed of a multitude of spectral bands pose a problem of representation. The technique of hyperspectral cube to generate a volumetric three-dimensional image (lines, columns and bands) can be an effective means of data representation.

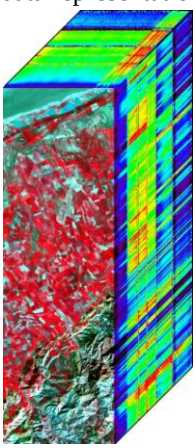

FIG. 2: REPRESENTATION MODE OF HYPERSPECTRAL DATA (HYPERSPECTRAL CUBE).

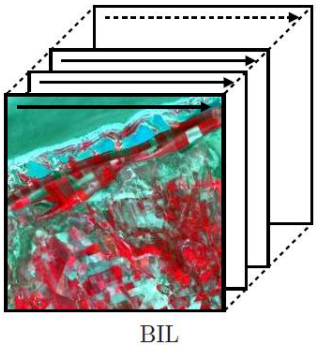

FIG. 3: ORGANIZATION OF THE PIXELS IN BIL FORMAT.

These images cover a surface area of 7.5 km by 100 Km. The spatial resolution is 30 meters and a spectral resolution of 10 nm, covering the spectral range from the visible (357 nm) to mid-infrared (2576nm). These images are delivered in raw format, each value is coded on 16 bits and the values are stored one after the other in Interleaved by Line Bits Format.

The scene used in this study was taken on 03/03/2003. They cover a part of the Mleta plain. By way of comparison, the same image of Landsat TM5 is presented with hyperspectral scene. This presentation gives a perfect idea between the two images in terms of spatial resolution.

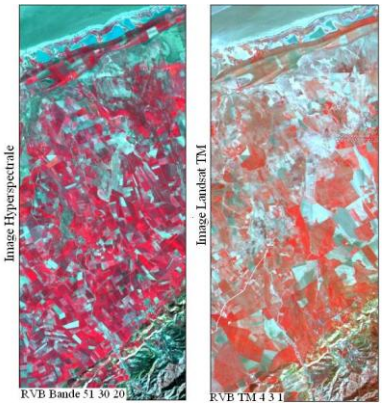

FIG. 4: COVERAGE SCENE OF THE STUDY AREA (RGB HYPERION AND TM IMAGES)

IV. TREATMENT OF THE HYPERSPECTRAL DATA

Some spectral bands of Hyperion sensor cannot be used. This is due to the absorption of all or most of the signal by some chemicals components present in the atmosphere such as H2O, CO, CO2.

Among the two hundred forty two (242) spectral bands, provided by the Hyperion sensor, only one hundred ninety eight (198) bands are calibrated. These bands have some defects due to defective sensor detectors. The visualization of each band is used to determine the affected columns for correcting or eliminate entirely noisy bands.

For many quantitative applications of remote sensing data, it is necessary to convert numbers into units representing the reflectance or current surface emission. The radiometric signal depends on the reflectance of the land surface but also the effects of the atmosphere during the round trip from sunlight.

The progress of the correction passes through two stages. The first step, the raw data expressed in numerical count (NC) is converted to reflectance measurement exo- atmospheric (sum of the reflectance of the earth and the atmosphere). It is obtained by a linear transformation of the numerical count to luminance (Wm-2sr-1 micron-1) by integrating the absolute calibration of the sensors gains. The second step is to subtract the atmospheric effects of the reflectance exo atmospheric.

4.1 Radiometric corrections

The calibrated data, which includes one hundred ninety eight (198) images, contains radiometric errors. The stripping phenomenon is different from one image to another. The absence of data or data deficient along a scan line is produced by system errors. The set of images have been processed one by one according to the degree and extent of scratches shown on each image. The most defective images have been excluded from the set. The technique used to correct these discontinuities observed on different images, is performed by replacing the missing pixel value by the average of the two neighboring pixels (left line with straight line).

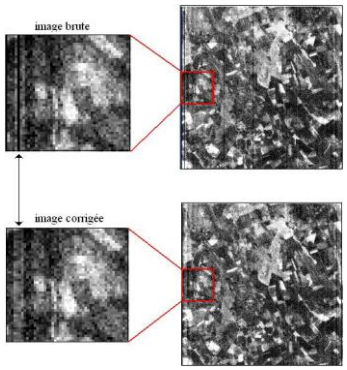

FIG. 5: TREATMENT OF THE STRIPES

4.2 Atmospheric corrections

The atmospheric corrections allow convert the acquired signal (radiance to the sensor or the electromagnetic energy received by the sensor) to a ground reflectance (actual energy reflected from the land surface), in order to compare the image spectral with terrain reference spectral or libraries spectral and to apply standardized treatment applicable only to reflectance data.

The atmospheric corrections were made using the model flaash (Fast Line-of-sight Atmospheric Analysis of Spectral Hypercubes) incorporated under the ENVI software. This model uses the MODTRAN radiative transfer code to calculate the reflectance. The model uses a correction approach using look-up tables (LUT) or five dimensions (Kaufman et al., 1997; Staenz et al, 2002), are the wavelength, the position of the pixel, the vapor atmospheric water, terrain height and optical thickness of the atmosphere.

The atmospheric correction process consists to convert the raw values expressed in numerical count (NC) to the radiance and reflectance by subtracting from it the disruptive effects caused by the atmosphere. The conversion of numerical accounts to radiance values is effected by taking into account the multiplication factors to express in a correct manner the reflectance measurements on the final image. The unit of measurement of the Hyperion data (correction level 1 b) is expressed in (w/cm2 micron SR *40) for visible and near-infrared channels and (w/cm2 micron SR *80) for the short infrared channels. The atmospheric correction module uses (micro W/cm2 nm SR). Thus, Hyperion image data will be multiplied by an extra

factor of 10. For this reason, the scaling factor used under FLAASH will be 400 for the visible and near-infrared channels and 800 for short infrared channels.

The conversion of the radiance measurements to the real reflectance is done by the FLAASH module. For that we have considered a standard mid-latitude summer atmosphere with continental aerosols (23 km visibility). The simulation is performed with MODTRAN the model.

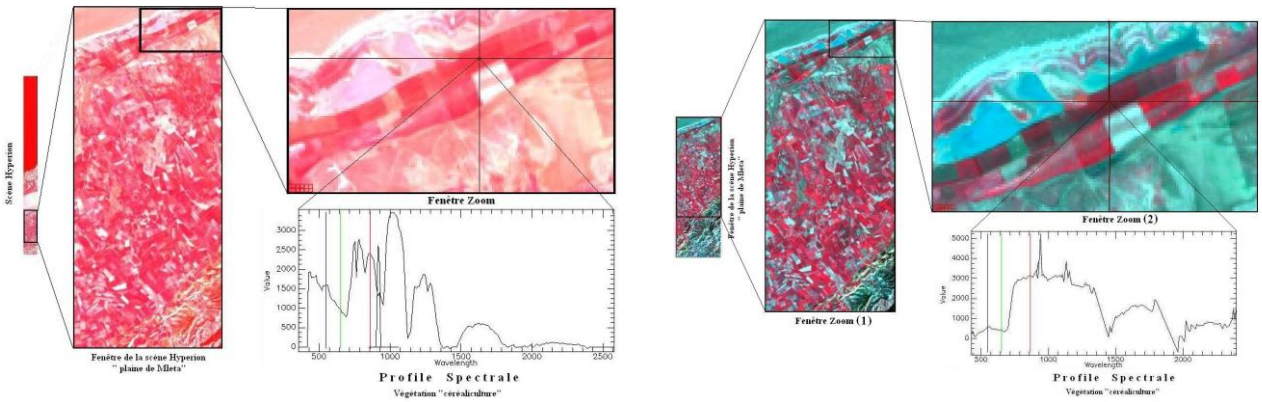

FIG. 6: THE HYPERSPECTRAL IMAGE BEFORE (LEFT) AND AFTER (RIGHT) THE ATMOSPHERIC CORRECTION

The result of the atmospheric correction, conducted by the FLAASH module, demonstrates that the vegetation spectrum taken as reference follows the exact spectral allure of a plant. To that effect, the atmospheric correction applied to the Hyperion images is significant.

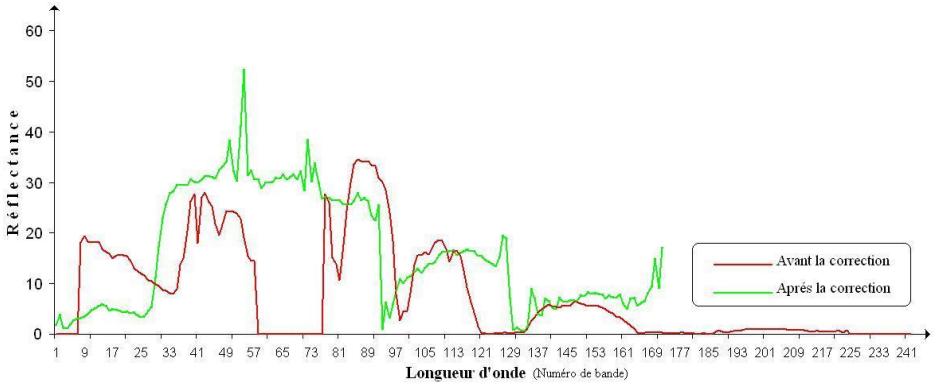

FIG. 7: VEGETATION SPECTRAL COMPARISON BEFORE AND AFTER THE ATMOSPHERIC CORRECTION

V. METHODS USED FOR MAPPING OF SALINE SOILS

The treatments of the spatial data are designed to extract the information contained in the image. The hyperspectral images are characterized by their large volume of data and the presence of noise. The classification methods based on classical statistics or those based on artificial intelligence (neurons network, cellular automata) are specific for multispectral images. New spectral classification methods have appeared (SAM, MTMF). They are based on spectral similarity and information at the subpixel level. These methods are developed in the context of the analysis of hyperspectral images, but they are also used in the multispectral field.

5.1 Application of the SAM method

The SAM classification method was developed by KRUSE and AL, (1993). It is based on a physical concept that measures the angular similarity of the spectral of each pixel in the image and reference spectral. These can be measured directly on the field as they can be extracted from the image itself. In multidimensional spectral space, the comparison between the two spectra allows to measure the angular deviation between them.

The attribution of a pixel in the image to a given class is based on the angle value which measures the similarity or the difference between the vector of the reference spectrum and its counterpart.

The subpixel classification, takes into account the value of the angle, the greater angle is small more the similarity between the spectrum of the evaluated pixel and the reference is greater. The spectral reference or spectral prototypes (endmembers) are determined from the image by the PPI Method.

The calculation of PPI requires in advance the calculation of the MNF components from a similar procedure of PCA (GREEN and AL, 1988). This transformation consists to minimize noise by compressing the information in a finite number of MNF elements (GREEN and AL, 1988; BOARDMAN and KRUSE, 1993).

5.2 Sequence of the processing steps

The MNF method is a variant of ACP adjusted to noise. This transformation is a rotation of the base in order to obtain a new orthogonal basis where the vectors are ordered following the report signal to noise (SNR) and not according to the variance as in the case of the PCA. It is used to reduce the dimension of hyperspectral data by separating the noise in the data. It is a linear transformation that is decomposed into two successive PCA followed by a normalization of noise. The first PCA is done compared to the statistics noise. At the end of this stage we get an orthogonal basis in which the noise is decorated. The intermediate base obtained at the end of this stage is the basis of eigenvectors of the noise covariance matrix. This basis is changed by a step for standardization to divide each vector by the root of its own value. The application of the MNF method on hyperspectral images allows eliminating noise and compressing the information on a limited number of images.

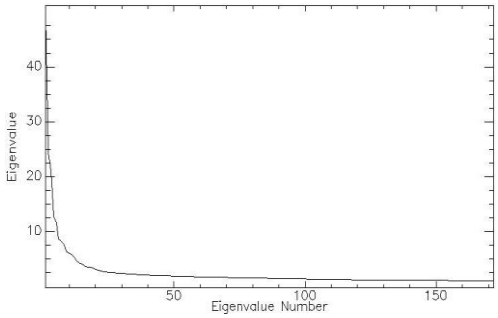

FIG. 8: SIGNIFICANT MNF BANDS

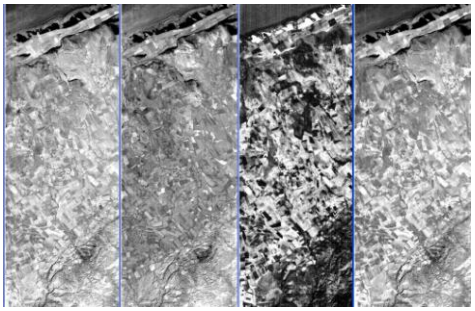

FIG. 9: THE FIRST FOUR (4) MNF BANDS

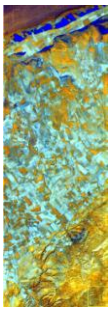

FIG. 10: THE THREE COLOR COMPONENTS OF MNF BANDS

The numbers of significant MNF bands carriers information are grouped in the first fifty seven (57) bands

The treatments with the three color components of the MNF images will allow highlight the salty soil. The lands affected by salts appear in the range of the blue color; this color encompasses the waters of depressions and hydrographic network (wadi) and some agricultural parcels.

5.3 Estimation of the Pixel Purity Index

The said PPI method is one of the prototypes signatures selection methods. It permits to identify spectrally pure pixels in remote sensing images. It's to produce an image where the pixel value represents the number of times that the pixel has been identified as extreme. These extremes represent pure pixels of the image (end members). The PPI is calculated on the fifty seven (57) MNF bands; pure pixels are identified and interpreted by their spectral signature. The procedure of the operation is performed by iterating through all of the pixels.

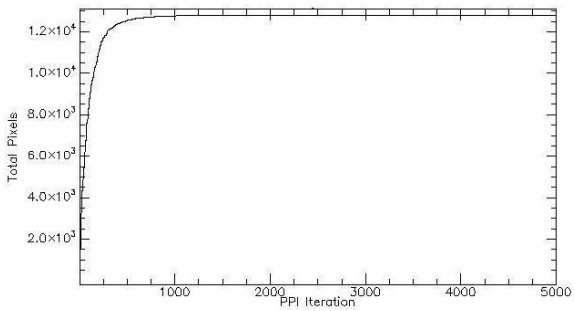

FIG. 11: THE PPI GRAPH

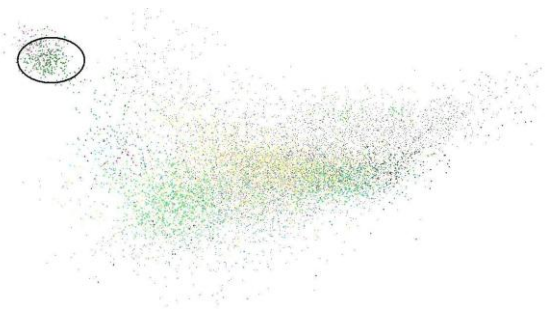

FIG. 12: MULTIDIMENSIONAL REPRESENTATION OF DIFFERENT SPECTRAL REFERENCE.

Significant numbers of the reference spectral of the different materials existing in the image was reconstructed from pure pixel. These spectral can be classified into clouds of points in multidimensional coordinate system. From the representation of the clouds of points in three dimensions (3D), we can easily define the representative classes in the hyperspectral image. These classes are usually located on the ends of the point clouds.

5.4 Classification of saline sols by the MNF method

This classification methodology is essentially based on the information in the various specters calculated from the image. To realize the classification of salted lands by the CASS method, we have selected the specters following the shape of the spectral response of halite. The comparison between the calculated spectrum from the image and that of halite (spectral library) shows a perfect similarity of these two spectral responses

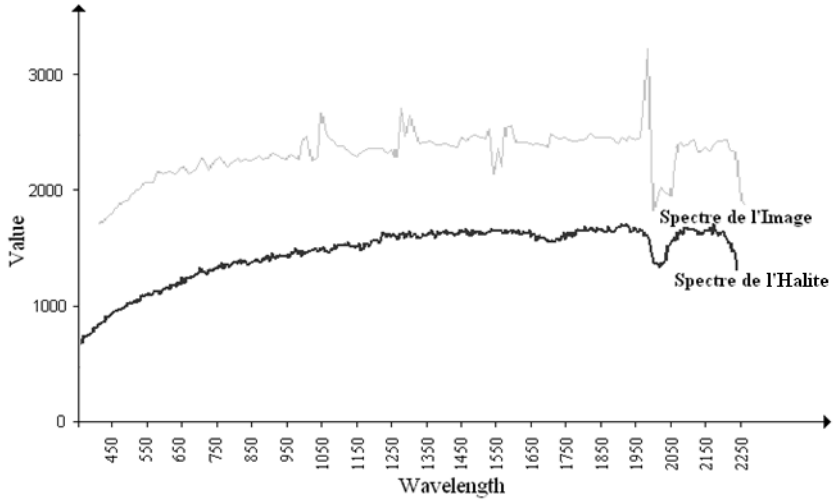

FIG. 13: SPECTRAL COMPARISON BETWEEN THE SPECTRUM OF HALITE AND THE IMAGE SPECTRUM

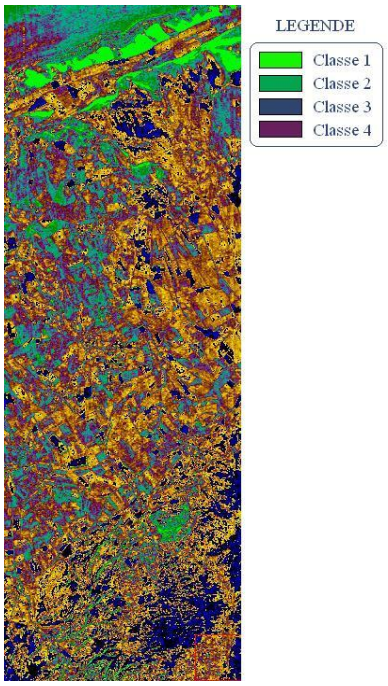

FIG. 14: IMAGE SAM CLASSIFIED

For saline soils cartography, classification by the SAM method was performed from different spectra that characterize soils contaminated. Four classes of saline soils have been identified on the result image.

VI. CONCLUSION

The use of the Hyperion hyperspectral imagery is growing and a wide field of application. They have the advantage to reproducing continuous spectral responses of the imaged objects.

In the field of photo-interpretation, the results indicate that hyperspectral satellite imagery is a source of reliable data for mapping the saline soil.

The different treatments applied to these images reveal interesting results in the localization and distribution of soil salt in the Mleta plain.

The results are very interesting, because knowledge of the spectral response of the salts present in the study area increases the quality and reliability of the used salinity mapping method.

REFERENCES

[1] Kaufman, Y. J., D. Tanre´, L. A. Remer, E. F. Vermote, A. Chu, and B. N. Holben, 1997: Operational remote sensing of tropospheric aerosol over land from EOS moderate resolution imaging spectroradiometer. J. Geophys. Res., 102, 17 051–17 067

[2] KRUSE, F.A., LEFKOFF, A.B., BOARDMAN, J.W., HEIDERBRECHT, K.B., SHAPIRO, P.J. AND GOETZ, A.F.H. (1993). « The spectral image processing system (SIPS) - interactive visualization and analysis of imaging spectrometer data. Remote Sensing of Environment ». vol. 44, n° 2-3, p. 145-163.

[3] Green, S., J. Boissoles, and C. Boulet, 1988: Accurate collision-induced line-coupling parameters for the fundamental band of CO in He: Close coupling and coupled states scattering calculations. J. Quant. Spectrosc. Radiat. Transfer, 39, 33-42.

[4] Staenz, K., Neville R.A., H.P. and White, S., 2002. Retrieval of Surface Reflectance From Hyperion Radiance Data, IEEE International Geoscience and Remote Sensing Symposium.